

PREPARED FOR SUBMISSION TO JINST

Scintillation characteristics of a NaI(Tl) crystal at low-temperature with silicon photomultiplier

H. Y. Lee^a J. A. Jeon^a K. W. Kim^a W. K. Kim^{b,a} H. S. Lee^{a,b} M. H. Lee^{a,b}

^a*Center for Underground Physics, Institute for Basic Science (IBS),
Daejeon 34126, South Korea*

^b*University of Science and Technology (UST),
Daejeon 34113, South Korea*

E-mail: kwkim@ibs.re.kr, hyunsulee@ibs.re.kr

ABSTRACT: Scintillation characteristics of a thallium doped sodium iodide (NaI(Tl)) crystal with a dimension of $0.6 \times 0.6 \times 2 \text{ cm}^3$ are studied by attaching a silicon photomultiplier (SiPM) direct to the crystal over a temperature range from 93 to 300 K. The scintillation light output and decay time are measured by irradiating 59.54 keV γ -rays from a ^{241}Am source. We observed approximately 20% increase in light yield at 230 K compared to that at the room temperature. At this condition, the NaI(Tl) crystal coupled with the SiPM can be a good candidate for future dark matter search detector.

Contents

1	Introduction	1
2	Experimental setup	2
3	SiPM only measurements	3
4	NaI(Tl)-SiPM measurements	5
5	Conclusions	9

1 Introduction

Due to excellent scintillation properties, NaI(Tl) crystals are widely used to measure energies of gammas from environmental radioactivities [1] and from interactions of new physics particles [2–7]. In particular, a direct detection of dark matter particles using NaI(Tl) crystal detectors is currently being conducted in several experiments [8–11]. The low-background NaI(Tl) crystals have been developed for a success of the dark matter detection at low energies by reducing internal radioactive contaminants in the crystal [12–15].

Conventional NaI(Tl) detectors are operating at the room temperature with photomultiplier tubes (PMTs) attached at each end of the crystal [8, 16]. On the other hands, PMTs are bulky and contain relatively large amount of radioisotopes [17, 18]. The photodetection efficiency (PDE) of the recently developed PMT, R12669SEL from Hamamatsu photonics, has the maximum value of 40% at around 420 nm corresponding to the emission peak of scintillation lights from the NaI(Tl) crystals. Silicon photomultipliers (SiPMs) could be good replacements of the PMTs because of their high PDEs for a broad range of wavelength and compact size with less radioactive materials [19]. A high dark count rate (DCR) of the SiPM was a contemporary problem for the application of the low-energy dark matter search experiment. However, DCR of the SiPM rapidly decrease at low temperatures [20]. A few experiments are conducting rare event searches using the SiPM already [21, 22].

Nonlinear temperature dependence of the NaI(Tl) crystals' scintillation light yield had been observed by a few measurements with PMT readout [23, 24]. Especially, increased light yields at temperatures around 150 and 250 K compared to that at the room temperature were reported [24]. In this case, the NaI(Tl) crystal coupled with the SiPM photosensor at the low temperatures can be an ideal combination for the dark matter search experiments. In this paper, we report responses of the NaI(Tl) crystal coupled with the SiPM sensor in a temperature range of 93 – 300 K and explore a possibility for the future dark matter search experiment.

2 Experimental setup

We use a NaI(Tl) crystal with a dimension of $0.6\text{ cm} \times 0.6\text{ cm} \times 2\text{ cm}$ that was cut from a crystal ingot grown in a program for the low-background NaI(Tl) development reported as NaI-036 in Ref. [14]. Several layers of soft polytetrafluoroethylene (PTFE) sheets were wrapped on side five faces of the crystal. The SiPMs from Hamamatsu photonics, model number S13360-6075CS with an active area of $0.6\text{ cm} \times 0.6\text{ cm}$, were attached to one side of the crystal. A micropixel size of $75\text{ }\mu\text{m} \times 75\text{ }\mu\text{m}$, a total of 6,400 micropixels, and a 50% PDE at 450 nm were provided in the specification by the company.

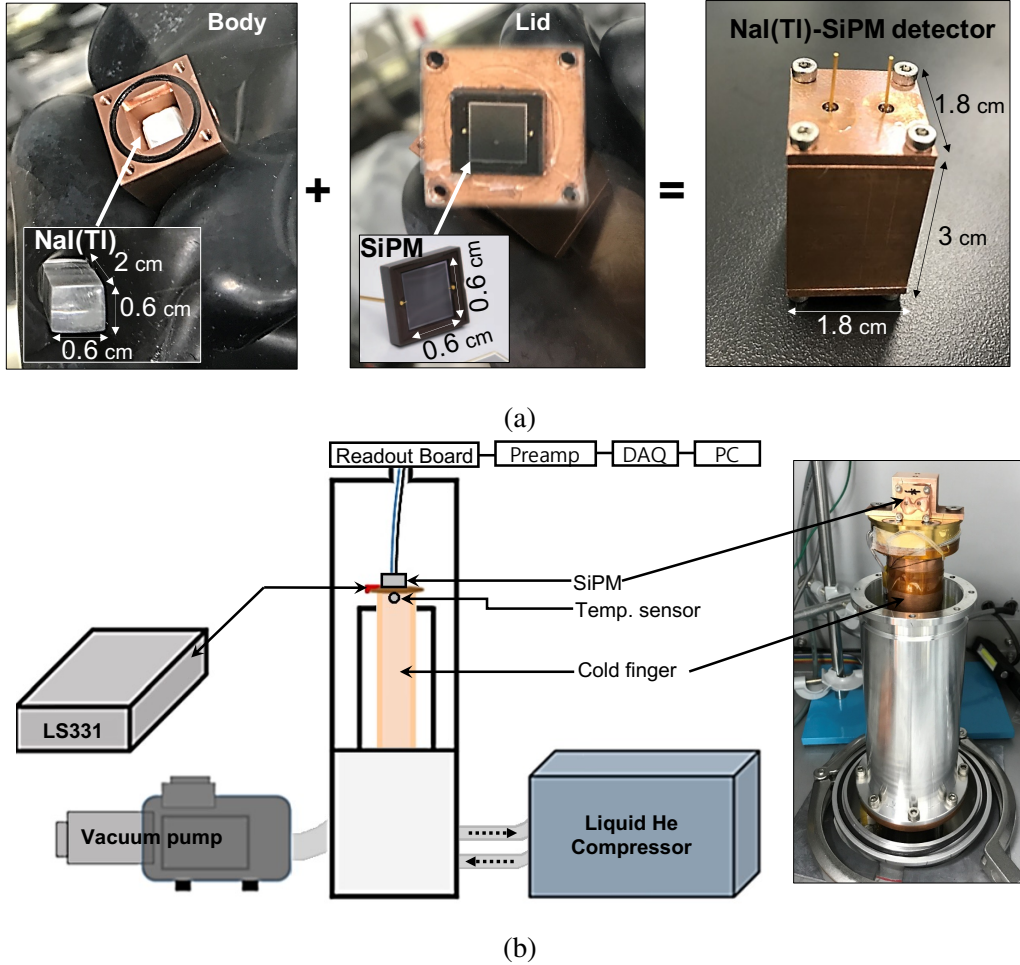


Figure 1. (a) NaI(Tl)-SiPM prototype assembly photos (b) Experimental setup for low-temperature measurements

The NaI(Tl) crystal was encapsulated in a copper housing to avoid moisture in the air due to its highly hygroscopic nature. The SiPM was coupled to the front face of the crystal in the housing named as "NaI(Tl)-SiPM prototype" as shown in Fig. 1 (a). The crystal was inserted into the housing and the SiPM was attached to the lid of the housing. The crystal and the SiPM had approximately 2 mm gap to maintain the same optical coupling condition. A Viton o-ring between the lid and the box was pressed with screws for an air tightness of the NaI(Tl) crystal. All assembly processes

were done inside a glove box in which the humidity level was maintained to be less than a few tens of ppm using N_2 gas and a molecular sieve trap. The dimension of the NaI(Tl)-SiPM prototype was $1.8\text{ cm} \times 1.8\text{ cm} \times 3\text{ cm}$ (W, D, H) as shown in Fig. 1 (a). A ^{241}Am source was placed above the copper housing to irradiate 59.54 keV γ -rays to the crystal.

The NaI(Tl)-SiPM setup was installed in a cryostat that could control the temperature from 4 K to the room temperature [25]. The schematic diagram of the cryostat is shown in Fig. 1 (b). A cold finger was cooled by a liquid helium compressor. The temperature of the cold finger was monitored by a silicon diode sensor and controlled through the Lakeshore LS331 temperature controller. The vacuum was maintained at approximately 10^{-2} Torr by a rotary pump. The NaI(Tl)-SiPM prototype was placed inside the thermal shield and directly attached to the cold finger. On the top of the NaI(Tl)-SiPM prototype, we installed one another temperature sensor. The detector was tested in a temperature range between 93 and 300 K of the cold finger. The experiment was performed at each temperature point after a few hours of waiting on the demanded temperature considering heat transfer to the crystal. Temperatures of the cold finger and the top of the NaI(Tl)-SiPM prototype were continuously measured and found about 3-5 K differences between two points that were accounted as a systematic uncertainty. The SiPM readout board was installed outside the cryostat. An amplified signal from the SiPM readout was digitized by a 125 MHz, 12-bit flash-analog-to-digital-converter (FADC). A $32\text{ }\mu\text{s}$ -long waveform was stored for each triggered event. Three different window types of resin, quartz, and windowless were tested for this measurement.

3 SiPM only measurements

A SiPM is a pixelated device where each micropixel is a series of an avalanche photodiode (APD) and a quenching resistor. The SiPM is externally biased with bias voltage V_{bias} so that the voltage on each APD is above its breakdown voltage V_{BD} . The difference $V_{bias} - V_{BD}$ is known as overvoltage ΔV which is one of the most important parameters affecting the performance of the SiPM.

To understand the characteristics of the SiPM, we first tested the SiPM without NaI(Tl) crystal in the cryostat. The V_{BD} was decreased at low temperatures [19, 26] because of ionization rate increase [27]. The results of increasing gain in the low temperature with the same V_{bias} are shown in Fig. 2. To avoid an impact caused by large gain changes from the temperature variation, we maintain ΔV equal to 3 V in the following measurements. Typically a single photoelectron (SPE) signal has a height of 12 mV and a width of 100 ns in this condition.

The SiPM exhibits several noise characteristics such as thermally generated DCR and pixel correlated cross talks. By maintaining ΔV equal to 3 V, we measure the DCR in a temperature range 90–300 K and an example charge distribution for that at the room temperature is shown in Fig. 3. A dramatic decrease of the DCR at low temperatures due to lower thermal generation probabilities [28] is shown in Fig. 4. From 300 to 140 K, the DCR decreases six orders of magnitude almost following an exponential function predicted by the Shockley-Read-Hall model [29]. DCR is about the same below 140 K that may be caused by band to band tunneling generation reported in Ref. [30].

Above 1.5 SPE charge accounts the rate of cross talks that generate multi-photoelectrons events as one can see in Fig. 3. When we evaluate the light yield of the NaI(Tl) crystal, the cross-talk rate is corrected to calculate proper number of photoelectrons. The cross-talk rate is known to be independent from the temperature with the same ΔV [19, 20], and we also observe a similar result.

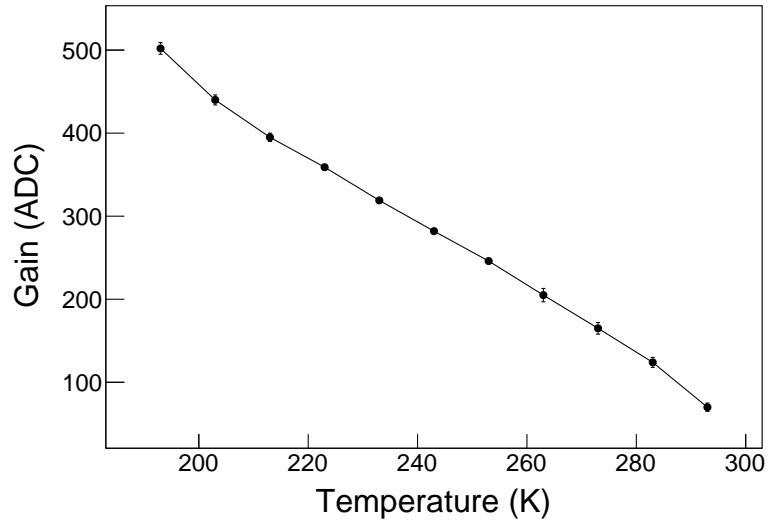


Figure 2. The SPE gain as a function of temperature with same V_{bias} of 54 V.

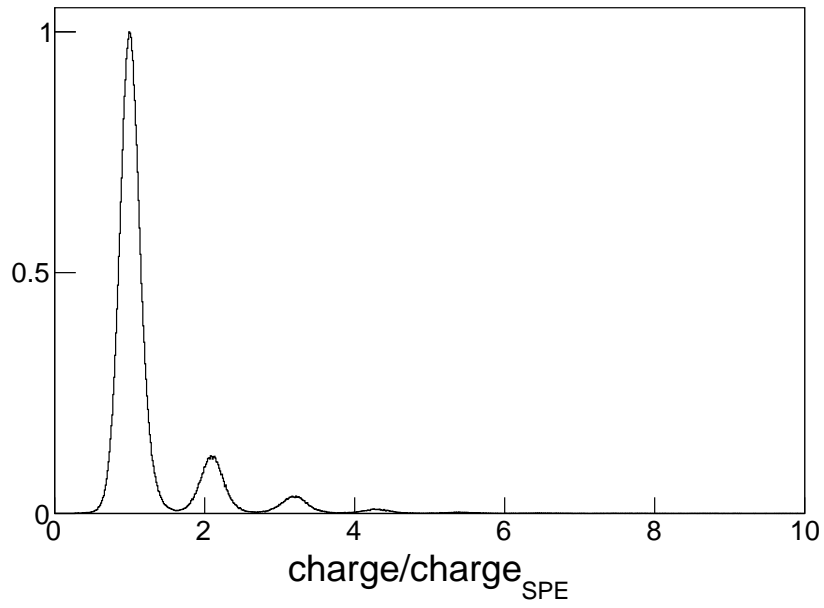


Figure 3. Charge distribution of the dark count events at the room temperature is presented. The typical dark current events provide a clear peak at single photoelectron but there are multi-photoelectrons events above 1.5 single photoelectron charge caused by cross talks.

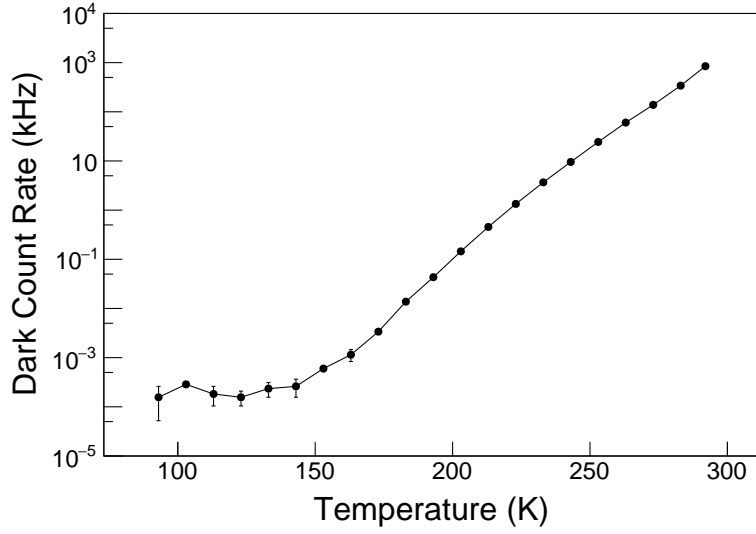


Figure 4. Dark count rates (DCR) in a temperature range 90–300 K while maintaining $\Delta V = 3$ V.

4 NaI(Tl)-SiPM measurements

After a characterization of the SiPM, we configured the NaI(Tl)-SiPM setup to measure light yields of the NaI(Tl) crystals at low temperatures. We irradiated 59.54 keV γ -rays from a ^{241}Am source and estimate a measured numbers of photoelectrons (NPE). The measured single photoelectron charge distribution in Fig. 3 is used to evaluate the light yield per keV together with the correction of the cross-talk rate. A contribution from DCR is also corrected by the temperature dependence measurement shown in Fig. 4. The distribution of NPE at the room temperature from the ^{241}Am source is shown in Fig 5. The root-mean-square resolution (σ/m) is obtained to 6.08 ± 0.06 %.

Figure 6 shows NPE as a function of the temperature relative to that of the room temperature (NPE_{room}). Three different SiPM windows are used for the measurements and show similar dependence of the light yield on temperature. Similar results using the PMT readout were reported previously [24]. The increased light yields of about 10–20 % at 220–250 K are consistent with Refs. [23, 24]. However, about 10% increased light yield at around 150 K using the PMT readout in Ref. [24] is not observed in the NaI(Tl)-SiPM setup although slightly increased light yield at around 120 K is presented in Fig. 6. A multiple different effects may be involed in this deviation including characteristics of different NaI(Tl) crystals, integration time window of each analysis [23], SiPM’s PDE depending on the temperature, and optical interfaces affected by temperature. Further study including PMT measurements and different crystals will help to understand this issue.

We have studied scintillation characteristics of the NaI(Tl) crystal as a function of temperature. Increased decay time of the NaI(Tl) crystal at low temperatures was already reported [23, 24]. Accumulated waveforms in different temperature measurements are modeled by two exponential functions as follows,

$$F(t) = b_1 \tau_f \exp^{-(t-t_0)/\tau_f} + b_2 \tau_s \exp^{-(t-t_0)/\tau_s} + bkg, \quad (4.1)$$

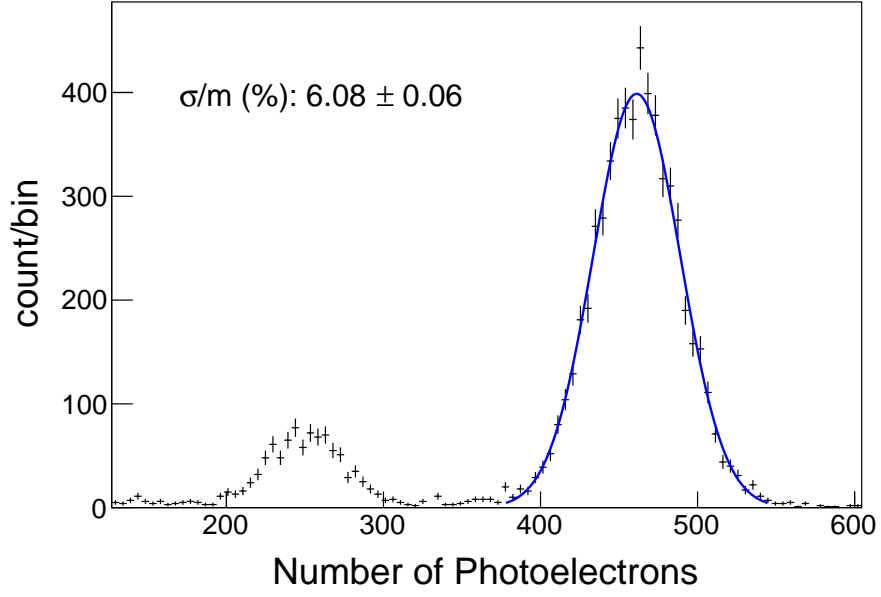


Figure 5. The measured NPE with the ^{241}Am source irradiating NaI(Tl) at room temperature is presented. The peak corresponding to 59.54 keV γ is fitted with a Gaussian function (blue solid line).

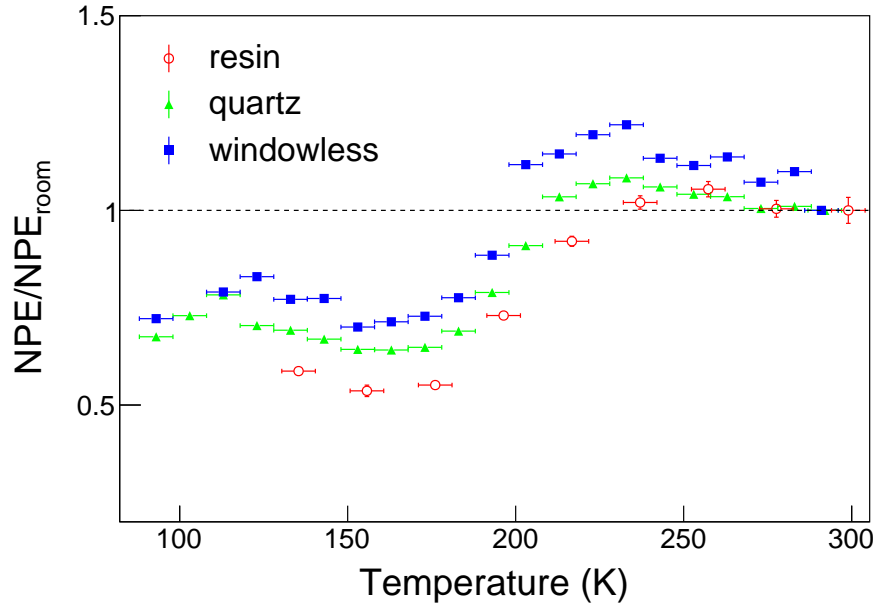


Figure 6. The measured NPEs as a function of temperature normalized to that at the room temperature (NPE_{room}) are presented for three SiPMs with different widow types.

where τ_f and τ_s are decay constants for fast and slow decaying components, and t_0 is the rising edge position. b_1 and b_2 are normalization factors and bkg represents continuum background from DCR. Figure 7 shows the accumulated waveforms of 59.54 keV gamma events for four selected temperatures of 293, 213, 173, and 113 K. Each waveform is fitted with Eq. 4.1 and fit results are overlaid.

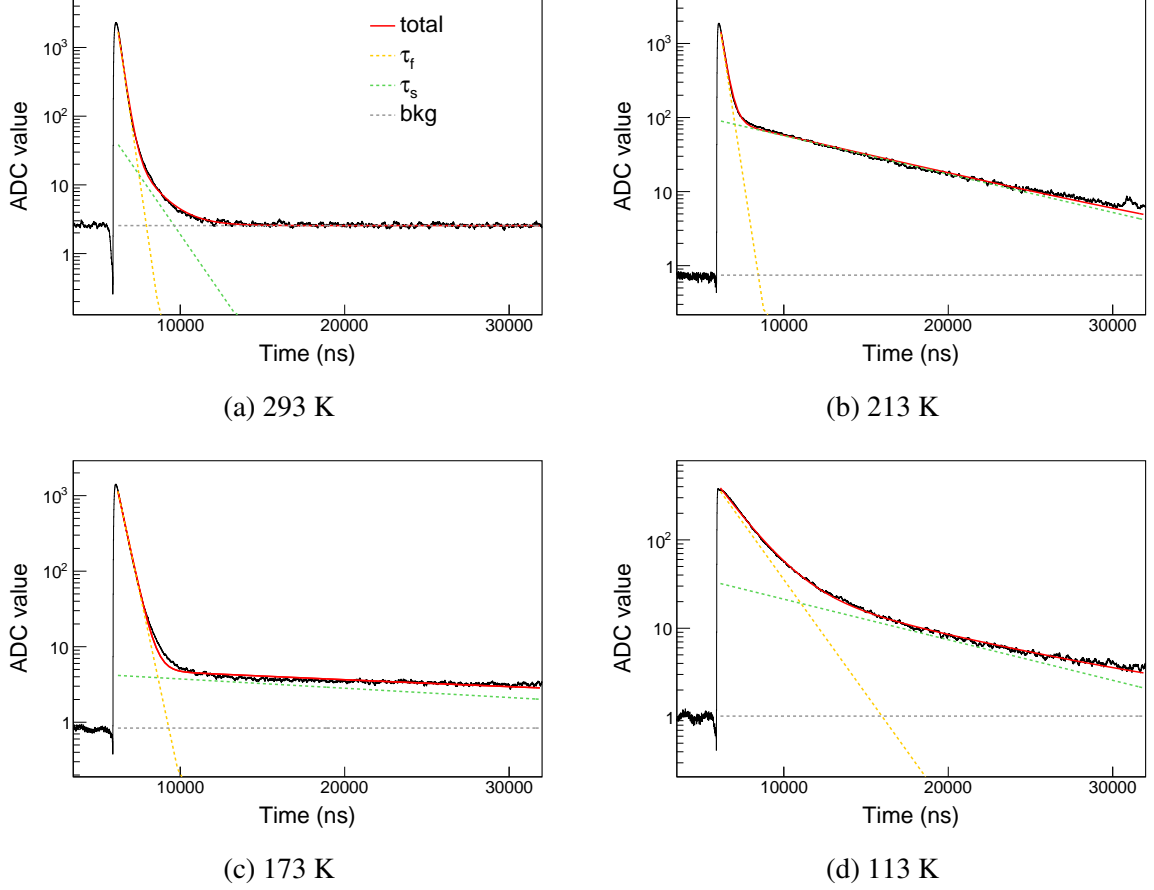


Figure 7. The accumulated waveforms of 59.54 keV gamma rays for four selected temperatures are presented. The red solid line shows the fitted results using two exponentials and a constant background. Each exponential and the constant background are separately overlaid in the plot.

The fast decay component at room temperature is approximately 240 ns that is consistent with previous measurements of about 220 ns [24, 31]. Slightly longer decay constants is expected due to about 100 ns width of the SPE pulse from SiPM. The decay constants for the fast component (τ_f) and the slow component (τ_s) are measured for a temperature range 93 – 300 K as shown in Fig. 8 (a). The relative amounts of the fast and slow components are shown in Fig. 8 (b).

As shown in Figs. 7 and 8, τ_s is getting slower below the room temperature down to 170 K. The relative ratio of the fast decay components are $87.8 \pm 4.6\%$, $38.6 \pm 3.2\%$, $87.3 \pm 4.2\%$, and $67.5 \pm 1.9\%$ for the temperatures of 293, 213, 173, and 113 K, respectively. The room temperature measurement with SiPM is consistent with previous measurements using PMTs [23, 31]. The reversed ratios of the fast and slow components around 240 K were observed in Ref. [32].

Maximum increase of the slow component at 230 K is observed as shown in Fig. 8 (b). Interestingly, this temperature has the maximum light yield of the NaI(Tl)-SiPM measurements as shown in Fig. 6. The two decay components correspond to the two different scintillation processes. The fast components are caused by the prompt capture of self-trapped excitons by the Tl level [23, 33]. Two competing processes to reach the activation centers of exciton by hopping and binary diffusion may cause the slow components [23, 33]. These process are highly depending on the temperature and therefore temperature dependent light yield of the NaI(Tl) crystals [23, 32, 33].

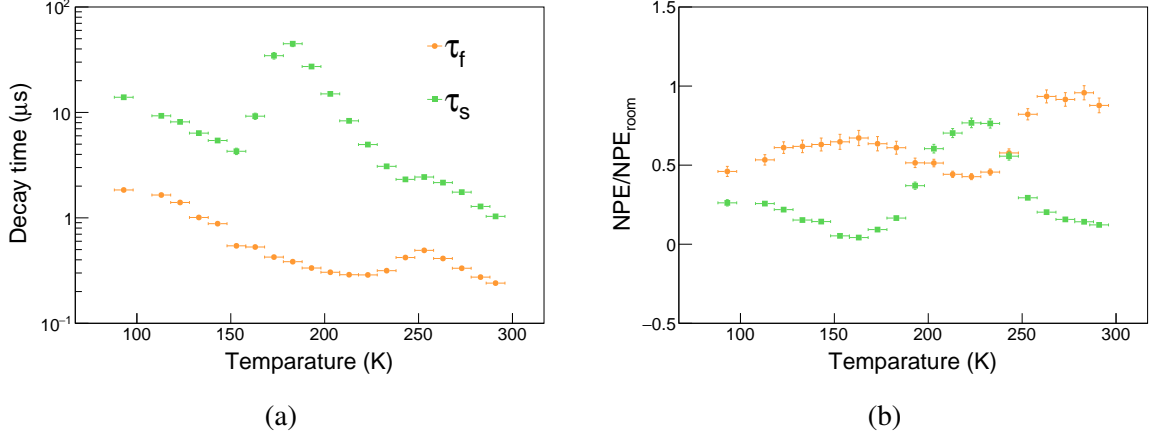


Figure 8. Decay time (a) and the fraction in the signal (b) of fast (yellow circle, τ_f), slow (green rectangular, τ_s) decay time in different temperatures.

We evaluate mean decay times of scintillation pulses in different temperatures defined as follows,

$$\text{Meantime} \equiv \frac{\sum_{i=0}^n h_i t_i}{\sum_{i=0}^n h_i} - t_0, \quad (4.2)$$

where h_i and t_i is the height and time of the i_{th} pulse, and t_0 is the time of the first pulse above the threshold. The meantime variables were open used to discriminate nuclear recoil events, which can be induced by dark matter interactions, from electron recoil backgrounds [5, 34]. Figure 9 shows the meantime as a function of temperature. Increased decay time from 0.3 to 4 μs is observed from room temperature to 210 K. Below this temperature, decreased decay time as low as 1 μs until 160 K is observed. This behavior may related with the observed light yields in Fig. 6. Increased light yields at around 220–250 K and decreased light yields at around 150–170 K are indeed correlated with amounts of the long-decay components as shown in Fig. 8. Because different nuclear recoil and electron recoil result in different ratios of the fast and slow decay components from different scintillation processes [35], the increased rate of the slow component from the electron recoil events at around 220 K may indicate improved pulse shape discrimination for the nuclear recoil events. Further investigation of the pulse shape discrimination using neutron irradiation at the low temperature is desired.

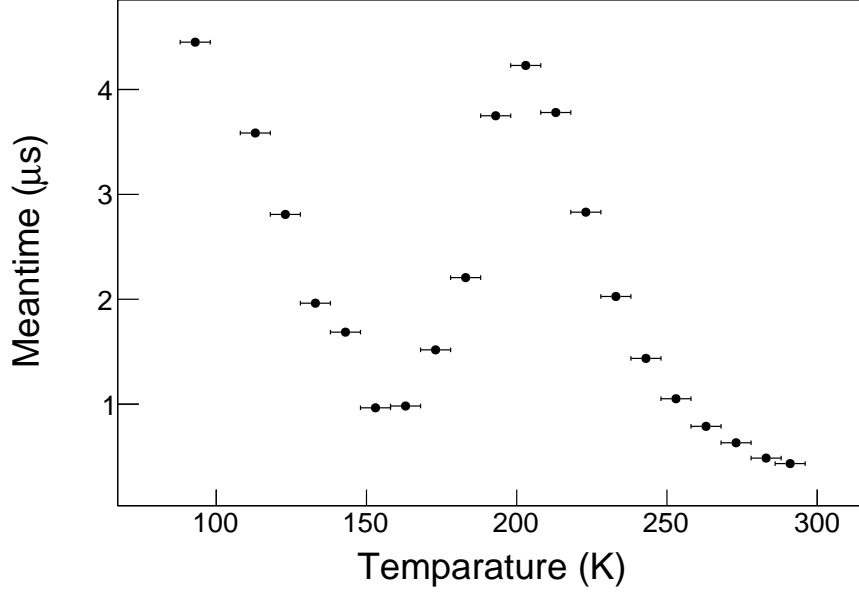


Figure 9. Mean time as a function of the temperature.

5 Conclusions

We have investigated characteristics of a few SiPMs at various temperature points from 300 down to 93 K. Significant decrease of dark count rate at low temperatures indicates that SiPM is a good photosensor for the dark matter search experiment at low temperatures. A NaI(Tl)-SiPM detector is also measured with the same temperature range to characterize the NaI(Tl) crystal's light yields and decay times. The light yield increased from 300 to 230 K with a maximal 20% relative to that of room temperature. In a similar temperature range, the ratio of the slow decay component is significantly increased. Considering increased light yield and decreased DCR, the NaI(Tl)-SiPM detector can be a good candidate detector for the future dark matter search experiment at low-temperatures.

Acknowledgments

This work is supported by the Institute for Basic Science (IBS) under project code IBS-R016-A1.

References

- [1] D. S. McGregor, *Materials for gamma-ray spectrometers: Inorganic scintillators*, *Ann. Rev. of Mater. Res.* **48** (2018) 245 [<https://doi.org/10.1146/annurev-matsci-070616-124247>].
- [2] S. Kim, H. Kim and Y. Kim, *Scintillator-based detectors for dark matter searches i*, *New J. Phys.* **12** (2010) 075003.
- [3] COSINE-100 collaboration, *An experiment to search for dark-matter interactions using sodium iodide detectors*, *Nature* **564** (2018) 83 [[1906.01791](https://doi.org/10.1038/s41586-018-0179-1)].

- [4] COSINE-100 collaboration, *Search for a dark matter-induced annual modulation signal in NaI(Tl) with the COSINE-100 experiment*, *Phys. Rev. Lett.* **123** (2019) 031302 [[1903.10098](#)].
- [5] KIMS collaboration, *Limits on Interactions between Weakly Interacting Massive Particles and Nucleons Obtained with NaI(Tl) crystal Detectors*, *JHEP* **03** (2019) 194 [[1806.06499](#)].
- [6] J. Amare et al., *First results on dark matter annual modulation from ANAIS-112 experiment*, *Phys. Rev. Lett.* **123** (2019) 031301 [[1903.03973](#)].
- [7] J. Amare et al., *Annual Modulation Results from Three Years Exposure of ANAIS-112*, *Phys. Rev. D* **103** (2021) 102005 [[2103.01175](#)].
- [8] COSINE-100 collaboration, *Initial Performance of the COSINE-100 Experiment*, *Eur. Phys. J. C* **78** (2018) 107 [[1710.05299](#)].
- [9] J. Amare et al., *Performance of ANAIS-112 experiment after the first year of data taking*, *Eur. Phys. J. C* **79** (2019) 228 [[1812.01472](#)].
- [10] SABRE collaboration, *The SABRE project and the SABRE Proof-of-Principle*, *Eur. Phys. J. C* **79** (2019) 363 [[1806.09340](#)].
- [11] R. Bernabei et al., *The DAMA project: Achievements, implications and perspectives*, *Prog. Part. Nucl. Phys.* **114** (2020) 103810.
- [12] K. Shin, O. Gileva, Y. Kim, H. S. Lee and H. Park, *Reduction of the radioactivity in sodium iodide (NaI) powder by recrystallization method*, *J. Radioanal. Nucl. Chem.* **317** (2018) 1329.
- [13] B. Suerfu, M. Wada, W. Peloso, M. Souza, F. Calaprice, J. Tower et al., *Growth of Ultra-high Purity NaI(Tl) Crystal for Dark Matter Searches*, *Phys. Rev. Research* **2** (2020) 013223 [[1910.03782](#)].
- [14] COSINE collaboration, *Development of ultra-pure NaI(Tl) detectors for the COSINE-200 experiment*, *Eur. Phys. J. C* **80** (2020) 814 [[2004.06287](#)].
- [15] K. Fushimi et al., *Development of highly radiopure NaI(Tl) scintillator for PICOLON dark matter search project*, *PTEP* **2021** (2021) 043F01 [[2101.00759](#)].
- [16] DAMA/LIBRA collaboration, *Performances of the new high quantum efficiency PMTs in DAMA/LIBRA*, *JINST* **7** (2012) P03009.
- [17] COSINE-100 collaboration, *Background model for the NaI(Tl) crystals in COSINE-100*, *Eur. Phys. J. C* **78** (2018) 490.
- [18] G. Adhikari et al., *Background modeling for dark matter search with 1.7 years of COSINE-100 data*, [2101.11377](#).
- [19] L. Baudis, M. Galloway, A. Kish, C. Marentini and J. Wulf, *Characterisation of Silicon Photomultipliers for Liquid Xenon Detectors*, *JINST* **13** (2018) P10022 [[1808.06827](#)].
- [20] P. K. Lightfoot, G. J. Barker, K. Mavrokoridis, Y. A. Ramachers and N. J. C. Spooner, *Characterisation of a silicon photomultiplier device for applications in liquid argon based neutrino physics and dark matter searches*, *JINST* **3** (2008) P10001 [[0807.3220](#)].
- [21] nEXO collaboration, *Sensitivity and Discovery Potential of nEXO to Neutrinoless Double Beta Decay*, *Phys. Rev. C* **97** (2018) 065503 [[1710.05075](#)].
- [22] DARKSIDE-20K collaboration, *DarkSide-20k: A 20 tonne two-phase LAr TPC for direct dark matter detection at LNGS*, *Eur. Phys. J. Plus* **133** (2018) 131 [[1707.08145](#)].
- [23] K. Ianakiev, B. Alexandrov, P. Littlewood and M. Browne, *Temperature behavior of nai(tl) scintillation detectors*, *Nucl. Instrum. Meth. A* **607** (2009) 432.

- [24] C. Sailer, B. Lubsandozhiev, C. Strandhagen and J. Jochum, *Low temperature light yield measurements in NaI and NaI(Tl)*, *Eur. Phys. J. C* **72** (2012) 2061 [[1203.1172](#)].
- [25] I. R. Pandey, J. Cheon, D. J. Daniel, M. Kim, Y. Kim, M. H. Lee et al., *A cryogenic setup for multifunctional characterization of luminescence and scintillation properties of single crystals*, *Rev. Sci. Instrum.* **91** (2020) 103108.
- [26] G. Collazuol et al., *Studies of silicon photomultipliers at cryogenic temperatures*, *Nuclear Instruments and Methods in Physics Research Section A: Accelerators, Spectrometers, Detectors and Associated Equipment* **628** (2011) 389.
- [27] S. M. Sze, Y. Li and K. K. Ng, *Physics of semiconductor devices*. John Wiley & sons, 2021.
- [28] A. Nepomuk Otte, D. Garcia, T. Nguyen and D. Purushotham, *Characterization of Three High Efficiency and Blue Sensitive Silicon Photomultipliers*, *Nucl. Instrum. Meth. A* **846** (2017) 106 [[1606.05186](#)].
- [29] W. Shockley and W. T. Read, *Statistics of the recombinations of holes and electrons*, *Phys. Rev.* **87** (1952) 835.
- [30] F. Acerbi, G. Paternoster, M. Capasso, M. Marcante, A. Mazzi, V. Regazzoni et al., *Silicon photomultipliers: Technology optimizations for ultraviolet, visible and near-infrared range*, *Instruments* **3** (2019) 15.
- [31] K. W. Kim et al., *Tests on NaI(Tl) crystals for WIMP search at the Yangyang Underground Laboratory*, *Astropart. Phys.* **62** (2015) 249 [[1407.1586](#)].
- [32] M. Moszynski, A. Nassalski, A. Syntfeld-Kazuch, T. Szczesniak, W. Czarnacki, D. Wolski et al., *Temperature dependences of $\text{LaBr}_3(\text{Ce})$, $\text{LaCl}_3(\text{Ce})$ and $\text{NaI}(\text{Tl})$ scintillators*, *Nucl. Instrum. Meth. A* **568** (2006) 739.
- [33] H. Dietrich, A. Purdy, R. Murray and R. Williams, *Kinetics of self-trapped holes in alkali-halide crystals: Experiments in $\text{NaI}(\text{Tl})$ and $\text{KI}(\text{Tl})$* , *Physical Review B* **8** (1973) 5894.
- [34] KIMS collaboration, *Pulse-shape discrimination between electron and nuclear recoils in a NaI(Tl) crystal*, *JHEP* **08** (2015) 093.
- [35] G. F. Knoll, *Radiation detection and measurement*. John Wiley and Sons, 2010.